Published by Carles Soriano, Guido Giordano, Ray Cas, Nancy Riggs, Massimiliano Porreca Facies architecture, emplacement mechanisms and eruption style of the submarine andesite El Barronal complex, Cabo de Gata, SE Spain
Journal of Volcanology and Geothermal Research, Volume 264, 15 August 2013, Pages 210–222
http://dx.doi.org/10.1016/j.jvolgeores.2013.07.001

Facies architecture, emplacement mechanisms and eruption style of the submarine andesite El Barronal complex, Cabo de Gata, SE Spain

Carles Soriano[a,*], Guido Giordano[b], Ray Cas[c], Nancy Riggs[d], Massimiliano Porreca[e,f]

[a] Institut de Ciències de la Terra Jaume Almera, CSIC, c/ Lluís Solé Sabarís s/n, Barcelona 08028, Spain, Tel. +34934095410, Fax +34934110012, E-mail: csoriano@ija.csic.es

[b] Dipartimento di Scienze Geologiche, Università degli Studi Roma Tre, Largo S. Leonardo Murialdo 1, 00146, Roma, Italy, E-mail: giordano@uniroma3.it

[c] School of Geosciences, Rm 128 Building 28 Clayton campus, Monash University, Victoria 3800, Australia, E-mail: Ray.Cas@sci.monash.edu.au

[d] Geology Program, School of Earth Sciences and Environmental Sustainability, Northern Arizona University, Flagstaff AZ 86011, USA, E-mail: nancy.riggs@nau.edu

[e] Centro de Vulcanologia e Avaliação de Riscos Geológicos (CVARG), Departamento de Geociências, Universidade dos Açores, Complexo Científico, 2º Piso, 9500-801 Ponta Delgada, Portugal, E-mail: Massimiliano.Porreca@azores.gov.pt

[f] Istituto Nazionale di Geofisica e Vulcanologia (INGV) - Sez. Roma 2
Via dell'Arcivescovado, 8
67100 L'Aquila – Italy; E-mail: massimiliano.porreca@ingv.it

Keywords: facies model, hyaloclastite, vesicular carapace, explosive subaqueous volcanism

Abstract

El Barronal complex consists of a succession of andesite lavas and andesite volcaniclastic facies interbedded with carbonate and siliciclastic sedimentary rocks. Carbonate and siliciclastic rocks were deposited in a shallow-marine environment during periods of volcanic quiescence. Lavas consist of an inner coherent core grading outward into hyaloclastite breccia made of dense clasts that in turn grade into hyaloclastite breccia made of vesicular clasts, in massive to layered zones. Volcaniclastic facies contain clasts produced during explosive eruptions and reworked clasts from sources above wave base. Volcaniclastic facies were deposited form cold granular flows with different grain size populations. Stratigraphy and facies architecture at El Barronal suggests that a succession of several discrete eruptive events occurred with a similar cyclic pattern made of an initial explosive phase followed by effusive emplacement of lavas, in turn followed by a period of quiescence of volcanic activity. Hyaloclastic fragmentation of magma took place in the final stages of lava emplacement, allowing only for local disorganization of the jigsaw-fit texture.

1. Introduction

The processes and products of subaqueous volcanism have been primarily studied in ancient volcanic successions (e.g. De Rosen-Spence et al. 1980; Yamagishi and Dimroth 1985; Cas et al. 1990; Kurokawa 1991; Goto and McPhie 1998; De Rita et al. 2001; Stewart and McPhie 2003; Nemeth et al. 2008), because of limited access to modern submarine volcanoes. The internal facies architecture of deposits erupted and emplaced in subaqueous conditions reflects the emplacement mechanisms and environmental conditions of submarine volcanism (i.e. water depth, effusion rate, magma volatile content, gas exsolution, magma composition; see Head and Wilson, 2003 and references therein).

Existing literature on subaqueous lavas deals mainly with two end-members: basaltic pillow lavas and felsic dome complexes. Subaqueous andesitic lavas typical may share characteristics of both pillow lavas and felsic domes (e.g. Bear and Cas 2007). Only a limited number of examples of andesitic lavas in subaqueous settings are known. They show that understanding their geometry and dimensions requires large and continuous exposures.

Here we present a reconstruction of the internal facies architecture of the Miocene andesitic El Barronal subaqueous volcanic complex (Cabo de Gata, SE Spain), where excellent and continuous exposures of a succession of thick lava units shed light on the emplacement mechanisms of viscous lava in a subaqueous environment. The internal architecture of the El Barronal volcanic complex is compared with other subaqueous lavas and domes in the literature. The general implications of the emplacement mechanism of lavas and the eruptive style of the El Barronal volcanic complex are discussed.

2. Geological setting

The Cabo de Gata volcanic zone is part of the Almeria-Níjar basin (Fig. 1), which is one of the intra-montane volcano-sedimentary basins forming the Alborán Domain, within the internal part of the Betic-Rif orogen (Montenat and Ott d’Estevou 1990; Sáenz de Galdeano and Vera 1992). The Cabo de Gata volcanic zone is a low-relief area with maximum altitudes of about 500 m asl (above sea level) that extends in a SW-NE direction from Cabo de Gata in the south to the north of Carboneras village (Fig. 1). The Cabo de Gata zone is bounded to the NW by the Carboneras Fault, a sinistral strike-slip structure that has been active from late Oligocene time to the present day (Scotney et al. 2000; Reicherter and Hübscher 2007). Outcrop stops to the SE at the coastline (Fig. 1).

The Cabo de Gata zone comprises interbedded volcanic and sedimentary rocks of Neogene age (Fernández Soler 1987; Serrano 1992; Martín et al. 1996; Montgomery et al. 2001). Sedimentary rocks are dominantly temperate-climate carbonate deposits, including also siliciclastic deposits (Martín 1996). Facies models and paleogeographic reconstructions of the fossiliferous carbonate rocks indicate a shallow-water submarine environment, above and below wave base (Serrano 1992; Martín et al. 1996, 2009; Johnson et al. 2005). Volcanic rocks are calc-alkaline, ranging in composition from basaltic andesite to rhyolite and volcanic facies have been interpreted to indicate submarine to emergent volcanic eruptions (Fernández Soler 1987, 2001; Di Battistini et al. 1987). Basement to the Neogene succession consists of Paleozoic and Triassic metamorphic rocks of the Alpujárride and Nevado-Filábride Complexes, and is exposed adjacent to the Cabo de Gata volcanic zone and along the Caboneras Fault zone (Fig. 1). The Neogene succession has not been metamorphosed and does not show internal deformation except in areas close to the Carboneras fault (Pedrera et al. 2006). The Neogene succession is affected by low-amplitude open folds with km-scale wavelengths and by subvertical normal faults (Arribas et al., 1995; Brachert et al. 2001; Pedrera et al., 2006). Eruptions were effusive and explosive, producing a wide variety of coherent and volcaniclastic facies. The original morphologies of volcanic edifices are poorly preserved due to erosion, although good sections of deposits occur in coastal cliffs and along incised valleys.

3. Volcanic stratigraphy of El Barronal area

The El Barronal area extends from Playa del Mónsul to Playa de Los Genoveses localities and is dominated by Cerro del Barronal, which faces south along the Mediterranean Sea yielding excellent exposures in coastal cliffs (Fig. 2). The area comprises three formations that are formally defined based on lithology, composition, and stratigraphic position.

3.1. Cerro Cañadillas Formation

The Cerro Cañadillas Formation crops out in the western part of El Barronal area, extending farther to the west of the Cabo de Gata volcanic zone (Fig. 2). It is the oldest unit (<12.6 Ma) in the area and comprises a succession of tabular lavas dipping to the E and NE. Bedded fiamme breccia occurs overlying some lava (Fig. 3). The minimum thickness of the Cerro Cañadillas Formation is 200 m. Lavas and fiamme breccia are dacitic in composition and have phenocrysts of feldspar, amphibole, biotite and quartz. Subvertical dikes up to 25 m wide and striking NNW-SSE intrude this unit and have the same phenocryst assemblage as the lavas. A fining-upward sedimentary sequence including massive conglomerate, parallel-bedded sandstone with shell fragments and ooids, and graded sandstone beds with swaley cross-stratification, overlies the Cerro Cañadillas pseudo-fiamme breccia at Playa del Monsul. This succession is in discordant contact with the overlying El Barronal Formation (Fig. 3).

3.2. El Barronal Formation

El Barronal rocks were characterized as pyroxene andesite lavas and dikes in early studies undertaken in the Cabo de Gata volcanic zone (Páez Carrión and Sánchez Soria 1965). Later on they were characterized as subaqueous lavas comprising coherent and hyaloclastite facies (Fernández Soler 1992; Fernández-Soler 2001).

El Barronal Formation consists of a succession of andesite lavas interbedded with andesite volcaniclastic deposits and carbonate and siliciclastic rocks. It extends from Playa del Mónsul to Morrón de Los Genoveses along the shoreline and farther inland to the NNW (Fig. 2). Volcaniclastic deposits are thin (< 20 m), whereas lavas form tabular bodies up to 60 m thick that are subhorizontal or dip shallowly to the east (Fig. 4). Lavas have a uniform andesitic composition with low alkali contents (<3 wt. % Na_2O+K_2O) and about 61 wt. % SiO_2 (Di Battistini et al. 1987). The upper boundary of El Barronal Formation is not exposed and the maximum exposed thickness is 150 m. We have performed $^{40}Ar/^{39}Ar$ dating in two distinct lavas at the Morrón de Los Genoveses locality (Fig. 2). The results of the isotopic dating are summarized in Table 1, and the stratigraphic positions of the dated lavas are shown in Figure 3. The isotopic age is 12.67+/-0.05 Ma for the lower lavas and 12.19+/-0.08 Ma for the upper lavas.

Lavas and volcaniclastic deposits of El Barronal Formation are intruded by subvertical dikes up to 50 m wide (Fig. 4) that strike NNW-SSE. Dikes are andesitic and have the same phenocryst assemblage as the lavas and volcaniclastic. The host rocks to dikes display irregular alteration halos up to tens of m wide that are characterized by a brownish color close to the dike margins that gradually turns into grayish and whitish away from the margins. The dikes have irregular glassy margins up to 40 cm wide.

Lavas and volcaniclastic facies are laterally continuous for more than 1 km and have been identified as andesitic (sub)units within El Barronal Formation, according to their stratigraphic position. For simplicity only lava (sub)units have been labeled in the figures (lava units 1 to 5). These (sub)units have been laterally correlated based on field mapping and stratigraphic position. Some lava units pinch out laterally in a succession of volcaniclastic facies (Fig. 4).

3.3. Los Genoveses Formation

Los Genoveses Formation crops out in coastal exposures at the Morrón de Los Genoveses and along Playa de Los Genoveses (Fig. 2). It consists of coherent rhyolite grading into rhyolitic pumice breccia. The exposed thickness of Los Genoveses Formation is 20 m. Coherent rhyolite consists of quartz, feldspar and biotite phenocrysts in a partly devitrified perlitic groundmass with flow foliation. Pumice breccia is clast-supported, although platy glass shards occur in the matrix. At the Morrón de Los Genoveses, coherent rhyolite intrudes lavas of El Barronal Formation dated in 12.67+/-0.05 Ma, and the contact is irregular and glassy (Fig. 3). Both coherent rhyolite and the El Barronal lavas are overlain by siliciclastic rocks containing rhyolite clasts and phyllite clasts from the metamorphic basement of the Cabo de Gata volcanic zone, and by upper lavas of El Barronal Formation dated in 12.19+/-0.08 Ma (Figs. 2 and 3).

4. Lithofacies of El Barronal Formation

Andesite lavas and andesite volcaniclastic facies are the main lithofacies of the El Barronal Formation, although interbedded carbonate and siliciclastic facies also occur. Carbonate and siliciclastic facies are described first to characterize the depositional environment of volcanism.

4.1. Carbonate and siliciclastic facies

It is beyond the scope of this contribution to undertake a detailed study of carbonate and siliciclastic facies. Only those features relevant to the El Barronal andesite volcanism are discussed. Carbonate and siliciclastic facies have discordant contacts with El Barronal lavas and volcaniclastic deposits. Carbonate rocks are cross-bedded coarse sandstone up to 2 m thick, containing shell fragments and volcanic clasts. Siliclastic rocks are polymictic, and contain rhyolite clasts, andesite clasts, and phyllite clasts from the metamorphic basement of the Cabo de Gata volcanic zone. Siliclastic rocks comprise sandstone and siltstone with cross- and plane-parallel beds and dm- to m-thick beds of breccia (Fig. 3).

4.1.1. Interpretation

The fossils and the sedimentary structures in the carbonate and siliciclastic facies are typical of shallow marine settings. This interpretation is in agreement with previous studies (e.g. Páez Carrión and Sánchez Soria 1965; Di Battistini et al. 1987; Serrano 1992; Fernández-Soler 2001). The non-volcanic character, occurrence of exotic clasts (shell, rhyolite, phyllite) and discordant contacts of carbonate and siliciclastic facies suggest interruptions in the andesitic volcanism and deposition of epiclastic facies.

4.2. Lava facies

Coherent and hyaloclastite facies are porphyritic to glomeroporphyritic with euhedral plagioclase, clinopyroxene, orthopyroxene and iron oxide phenocrysts in a partly devitrified groundmass with plagioclase microlites and pyroxene and iron oxide crystals. Coherent facies are surrounded by hyaloclastite facies along gradational contacts (Figs. 3 and 4). At these contacts, coherent facies are pervasively fractured. Hyaloclastite facies are volumetrically dominant in the El Barronal complex. They are monomictic breccias made of clasts ranging in size from 1 cm to 1 m and show clast-supported domains grading into matrix-supported domains. Jigsaw-fit texture is ubiquitous and grades into domains in which clasts are slightly rotated. Two types of coherent facies and three types of hyaloclastite facies are distinguished.

4.2.1. Colonnade columnar-jointed facies

Colonnade columnar-jointed facies is a coherent facies characterized by subvertical columnar joints and subhorizontal flow bands. Columnar joints form pentagonal to hexagonal prisms up 15 cm in diameter. This facies has a sheet morphology that extends for up to 1 km and a thickness that ranges from 10 to 30 m. This facies occurs in lava units 2, 4 and 5 of El Barronal Formation.

4.2.2. Entablature columnar-jointed facies

Entablature columnar-jointed facies is a coherent facies consisting of columnar, slightly curved, joints that exhibit a fan-like pattern and form rosette structures. Locally, entablature columnar-jointed facies shows flow bands perpendicular to the columnar joints. Rosettes are isolated structures up to 20 m in radius and also form piles in which individual rosettes have a maximum radius of 2 m (Fig. 5). Rosette structures are preferably exposed on NW-SE surfaces roughly perpendicular to the ENE-WSW trend of the coastline. This facies ranges in thickness from 5 to 25 m and occurs in lava units 1, 3 and 4.

4.2.3. Massive hyaloclastite breccia with dense clasts

Massive hyaloclastite breccia with dense clasts is clast-supported and lacks internal organization (Figs. 5 and 6). Clasts are black, glassy, angular and dense and the matrix is minor (<40 %), although coastal weathering has enhanced a matrix-supported appearance and makes clasts appear to be locally subrounded. Clasts are subequant with curviplanar edges and the matrix is composed of smaller clasts (>1 cm) of identical composition to larger clasts; the smaller clasts also have jigsaw-fit texture. Massive hyaloclastite breccia ranges in thickness from 0.5 to 20 m and grades into colonnade-jointed and entablature-jointed coherent facies and into massive hyaloclastite breccia with vesicular clasts and into layered hyaloclastite breccia (Figs. 5 and 6).

4.2.4. Massive hyaloclastite breccia with vesicular clasts

Massive hyaloclastite breccia with vesicular clasts is a non-organized breccia in which vesicular clast are dominant and dense clasts are subordinated (<50%). Vesicular clasts have poorly defined outlines (ghosts of vesicular clasts) and fit together. Dense clasts (>2 cm) are embedded in a fine (<2 mm) whitish groundmass yielding a matrix-supported appearance (Fig. 6). This matrix-like groundmass is porphyritic and consists of phenocrysts in a partly devitrified groundmass with plagioclase microlites and up to 40% of glassy vesicles. Jigsaw-fit texture has been also observed in the matrix-like groundmass. Vesicles are subspherical to elongate, have glassy vesicle walls and vesicle diameter ≤100 μm. Some vesicles accommodate the shape of phenocrysts whereas others accommodate the shape of neighboring vesicles (Fig. 6B). Massive hyaloclastite breccia with vesicular clasts has irregular, abrupt and gradual contacts with massive hyaloclastite breccia with dense clasts and occurs in lava unit 1 (Fig. 6A, C). It ranges in thickness from 0.5 to 20 m.

4.2.5. Layered hyaloclastite breccia

Layered hyaloclastite breccia is defined by the alternation of bands of massive hyaloclastite breccia with dense clasts and bands of massive hyaloclastite breccia with vesicular clasts (Figs. 7 and 8). Bands are cm to dm thick, slightly undulating and laterally discontinuous, grading laterally into massive hyaloclastite breccia facies. Contacts between bands are gradational to abrupt. Jigsaw-fit to clast-rotated texture is common within both types of bands (Figs. 7B). Bands of massive hyaloclastite breccia with vesicular clasts have elongate vesicles with long/short axes ratio <5 aligned parallel to phenocrysts and presumably parallel to the bands (Fig. 8B). In lava units 2 and 3, layered hyaloclastite breccia grades into massive hyaloclastite breccia with dense clasts and then into coherent facies. In lava unit 2, bands dip gently toward the ESE and are concordant with flow bands in the lower colonnade jointed facies (Fig. 8A). In lava unit 3, bands are subvertical and this facies grades laterally toward the west into massive hyaloclastite breccia with dense clasts and into entablature jointed facies (Fig. 7A). Thickness of layered hyaloclastite breccia ranges from 10 to 25 m.

4.2.6. Interpretation

Subequant clasts with curviplanar edges, widespread jigsaw-fit to clast-rotated textures and glassy texture indicate that breccias originated from the quenching and emplacement of hot magma in subaqueous conditions (Fernández Soler 1992; Fernández-Soler 2001). The monomictic nature of hyaloclastite breccia, the identical compositional and textural character of the breccia and the coherent facies and gradational contacts of breccia into coherent facies indicate a co-genetic origin of coherent and hyaloclastite facies.

Massive hyaloclastite breccia with dense or vesicular clasts is inferred to form by quench fragmentation of hot andesite comprising dense or vesicular domains, whereas layered breccia is interpret to reflect quench fragmentation of vesicular and non-vesicular bands. Vesicular bands contain elongate vesicles likely deformed by simple and pure shear in a laminar flow. Therefore, layered hyaloclastite breccia is interpreted to reflect original flow bands defined by the degree of vesiculation.

Coherent facies grades outward into hyaloclastite facies indicating that coherent facies forms the interior of lavas and hyaloclastite facies forms the external part of lavas. The disposition of columnar joints in coherent facies is perpendicular to the cooling surface defined by of the outer hyaloclastite breccia. Rosette structures in coherent facies are dominantly oriented on NW-SE surfaces and suggest that they are cylindrical structures rather than spherical and that the cylindrical axis is roughly ENE-WSW. Single lava units, including both coherent and hyaloclastite facies, vary in thickness from 40 to 60 m thick. Their lateral extent of 1-2 km along sea cliff exposures suggests an apparent aspect ratio from 1/50 to 1/30. These aspect ratios suggest that the El Barronal lava units correspond to tabular bodies rather than to dome structures.

4.3. Bedded andesite volcaniclastic facies

The El Barrronal volcaniclastic facies are composed of andesititc clasts that vary in terms of texture, vesicularity, color and rounding. They are consolidated rocks forming beds with different internal organization, grain size and componentry and are interbedded with andesite lavas. The phenocryst assemblage of clasts in volcaniclastic facies is identical to that of the lavas. Volcaniclastic facies show significant lateral and vertical variations in facies and thickness; the coarser facies corresponding to the thicker accumulations and the finer facies corresponding to the thinner. Thicknesses of volcaniclastic facies range from 0.5 to 20 m. Volcaniclastic facies exhibit rapid vertical and lateral gradations of facies. Four types of volcaniclastic facies have been distinguished.

4.3.1. Massive breccia

Massive breccia is clast to matrix supported and poorly sorted, consisting of angular to subangular clasts ranging in size from a few cm to up to 2 m across (Fig. 9A). Two types of clasts are distinguished: dense clasts (>50 vol. %), typically black and glassy but also gray and reddish, and vesicular clasts, typically white and glassy. Vesicular clasts are less abundant and locally more rounded than dense clasts. They are poorly vesicular (vesicles <40 vol. %); elongate vesicles have long/short axes ratio <5. Matrix is coarse (>2 cm) and vesicular clasts are dominant, although it also contains dense clasts and a few crystals. Beds are internally massive, decimeter to meter thick and laterally restricted (<10 m). Some beds are weakly inversely and normally graded. Beds of massive breccia have erosive bases and also show convex upward geometry and terminate abruptly (Fig. 9C).

4.3.2. Diffusely bedded pumice-rich breccia

Diffusely bedded pumice-rich breccia is a poorly sorted clast-supported aggregate of pumice clasts, dense clasts and crystals, and contains outsized dense clasts up to 1 m across (Fig. 10A). This facies shows plane parallel and low-angle cross-beds and distorted beds. Beds range from a few cm to a few m thick and are laterally discontinuous. Pumice clasts are dominant (>50 vol. %), porphyritic, highly vesicular (vesicles >60 vol. %) and have tube vesicles showing long/short axes ratio >10. Pumice clasts are centimeter in diameter, angular to sub-rounded and show random orientation of the tubes in adjacent clasts (Fig. 10B). The edges of pumice clasts cut the tubes at high angles and are parallel to the tubes (Fig. 10B). Dense clasts are reddish, greenish, gray, black and glassy, and sub-angular to well rounded (Fig. 10A). Matrix (<2 mm) is rare and contains pumice clasts, crystals, dense clasts and platy, cuspate and bubble-wall glass shards (<5 vol. %) less than 250 μm in diameter (Fig. 10C). This facies is interbedded with thinly bedded fine tuffaceous sandstone showing gradational contacts.

4.3.3. Cross-bedded crystal-rich sandstone

Cross-bedded crystal-rich sandstone is gray and moderately sorted with low-angle cross-bedded. It consists of up to 50 vol. % crystals and crystal fragments and up to 30 vol. % dense clasts. Crystals of plagioclase, pyroxene and iron oxides are sub-angular to sub-rounded, many of them have a blocky shape and some pyroxene crystals have a reddish coating. Dense clasts are gray, brown and reddish, sub-angular to well-rounded and have perlitic cracks (Fig. 11A). Beds of this facies range from mm to up to 50 cm thick and may show inverse and normal grading and outsized clasts that form trains or isolated clasts. Beds are distorted and show small-scale faults and folds.

4.3.4. Thinly bedded fine tuffaceous sandstone

Thinly bedded fine tuffaceous sandstone consists of well sorted, mm- to dm-thick beds that contain crystals and crystal fragments (up to 30 vol. %), dense clasts (20 vol. %), pumice clasts (10 vol. %), glass shards (<10 vol. %) and rare unidentified bioclasts (Fig. 11B). Some beds are normally graded; other show cross-lamination and low-angle truncations. Beds contain outsized dense and vesicular clasts (<50 cm) forming trains and as isolated clasts (Fig. 9B). Beds have mm- to cm-scale faults and folds, dish structures and distorted lamination under the load of outsized clasts and large clasts in upper volcaniclastic beds (Fig. 9B). Crystals and dense fragments are usually blocky, similar to those of the cross-bedded crystal-rich sandstone facies (Fig. 11B). Pumice clasts are highly vesicular (vesicles >60 vol. %) and have tube vesicles; glass shards are platy, cuspate and bubble shape (Fig. 11B). This facies shows rapid vertical and lateral gradations into massive breccia and cross-bedded crystal-rich sandstone (Fig. 9C).

4.3.5. Interpretation

Andesite volcaniclastic facies are interbedded with hyaloclastite lavas suggesting a subaqueous depositional environment. Hot emplacement structures (i.e. degassing pipes, welding, columnar joints) have not been observed and tractive structures and grading are common, indicating that andesite volcaniclastic facies were deposited from cold flows. Distorted bedding, small-scale faults and folds and dish structures are soft-sediment deformation structures (rather common in the finer andesite volcaniclastic facies) suggesting that volcaniclastic facies were water-saturated when deformed and, given the subaqueous deposition, likely at emplacement.

Andesite volcaniclastic facies lack fine matrix (< 0.05 mm) and the matrix below 2 mm is rare in the diffusely bedded pumice-rich breccia. Beds of volcaniclastic facies are internally organized (massive breccia shows weak grading) and tractive structures are common. These features allow interpreting the andesite volcaniclastic facies collectively as deposited from granular and non-cohesive flows with different grain size populations. Absence of fine matrix and dominant clast-supported nature of volcaniclastic facies suggest grain-to-grain support mechanisms. Nevertheless, water support mechanisms cannot be excluded, given the subaqueous emplacement and that the sorting and tractive structures observed in the finer volcaniclastic facies can be attributed to dilute flows.

Highly vesicular pumice clasts with tube vesicles have clast edges parallel and at high angles to the tubes. Similar pumice clasts have been described in many magmatic explosive eruptions in which magma fragmentation occurs in the volcanic conduit (Marti et al. 1999; Polacci et al. 2003; Rosi et al. 2004). Therefore, we interpret tube pumice clasts in the diffusely bedded pumice-rich breccia and the thinly bedded fine tuffaceous sandstone as fragmented during magmatic explosive eruptions. Glass shards of ash size can be produced by a number of different processes including abrasion during transport (Manga et al. 2011). However, bubble-wall, platy and cuspate shards have been also interpreted elsewhere as produced by the explosive fragmentation of magma and, given that they co-exists with tube pumice clasts in the diffusely bedded pumice-rich breccia and the thinly bedded fine tuffaceous sandstone, this seems a reasonable interpretation. The blocky shape of some dense fragments and many crystals and in the cross-bedded crystal-rich sandstone and thinly bedded fine tuffaceous sandstone could be attributed to magma-water interaction processes during explosive fragmentation of magma. Magma-water interaction enhances fragmentation efficiency and could be also responsible for the fine grain size of these facies.

Poorly vesicular clasts with vesicles showing low long/short axes ratio (<5) are significantly different from highly vesicular clasts with tube vesicles. Poorly vesicular clasts and dense clasts in the volcaniclastic facies are compositionally and texturally similar to the coherent and hyaloclastite facies of lavas. Hence, they are interpreted to have been derived from underlying lava units. Differences in rounding and in color of dense clasts suggest different provenances. Well-rounded clasts can be attributed to sources above wave base and the reddish color of some clasts to oxidizing conditions. Clast rounding suggests reworking and, together with oxidation, may occur during periods of volcanic repose.

4.4. Contact relations between andesite lavas and andesite volcaniclastic facies and distribution of andesite volcaniclastic facies

In lava unit 1, massive hyaloclastite breccia with vesicular clasts grades downward into massive hyaloclastite breccia with dense clasts and into coherent facies (Fig. 6A). The upper part of the massive hyaloclastite breccia with vesicular clasts contains scattered domains of cross-bedded crystal-rich sandstone (Fig. 6A). The domains are irregularly distributed about 10 m above the contact to the lower massive hyaloclastite breccia with dense clasts and 5 m below the contact to upper bedded andesite volcaniclastic facies. Cross-bedding is not parallel across different the domains and it is not parallel to bedding of upper andesite volcaniclastic facies. These domains have an irregular shape and are up to a few decimeters across, and the contacts with the surrounding massive hyaloclastite breccia with vesicular clasts are abrupt and diffuse (Fig. 6A). Diffuse contacts are defined by a zone of variable thickness in which cross-bedding cannot be observed and irregular to blocky portions of massive hyaloclastite breccia with vesicular clasts are intimately mingled with portions of cross-bedded crystal-rich sandstone at millimeter to centimeter scale (Fig. 6D). Massive breccia with vesicular clasts is overlain on a sharp contact by andesite volcaniclastic facies including beds of massive breccia and cross-bedded crystal-rich sandstone. These beds onlap the upper boundary of massive breccia with vesicular clasts.

In lava unit 3, subvertical bands in layered hyaloclastite breccia are truncated by subhorizontal beds of overlying thinly bedded fine tuffaceous sandstone (Fig. 7C). Laminae in the thinly tuffaceous sandstone are distorted, typically concave upward, beneath clasts of the overlying massive hyaloclastite breccia with dense clasts in lava unit 4. Distorted and concave upward laminae are also observed at the contact between thinly bedded fine tuffaceous sandstone and the overlying massive breccia with dense clasts of lava unit 3 (Fig. 12). At this contact, some hyaloclasts appear to have sunken into the underlying thinly bedded fine tuffaceous sandstone.

At Playa del Barronal, lava unit 3 tapers and pinches out toward the W, leaving lava unit 4 on lava unit 2 in a succession of andesite volcaniclastic facies that thickens toward the SE (Fig. 4). The succession overlies the massive hyaloclastite breccia with dense clasts in lava unit 3 with a poorly exposed contact. The succession consists of tightly interbedded beds of massive breccia, thinly bedded fine tuffaceous sandstone and cross-bedded crystal-rich sandstone. Beds of these facies have gradational contacts and show rapid lateral and vertical transitions among them (Fig. 9C). Farther to the east near, Morrón de Los Genoveses, andesite volcaniclastic facies consist of diffusely bedded pumice-rich breccia interbedded with thinly bedded fine tuffaceous sandstone showing gradational contacts with rapid lateral and vertical transitions. The andesite volcaniclastic succession at Morrón de Los Genoveses is overlain on a poorly exposed contact by massive hyaloclastite breccia with dense clasts in lava unit 4 and it overlies siliciclastic rocks with a discordant contact. Beds of the andesite volcaniclastic succession dip moderately to the south whereas siliciclastic rocks dip moderately to the east (Fig. 2).

4.4.1 Interpretation

Diffuse contacts of domains of cross-bedded crystal-rich sandstone showing irregular to blocky portions of massive hyaloclastite breccia with vesicular clasts intimately mingled below a centimeter scale with sandstone in which cross bedding is no longer observed can be interpreted as peperite produced by disintegration of hot magma at the contact to water-saturated volcaniclastic sand (cf. Skilling et al. 2002 and references therein). Sandstone domains are irregularly distributed in the uppermost part of lava unit 1, they do not grade upward into the bedded andesite volcaniclastic facies and the cross-bedding of domains, when preserved, is not parallel to bedding of the upper andesite volcaniclastic facies. For these reasons, lava unit 1 being partly intrusive seems a plausible interpretation.

Distorted lamination in the fine volcaniclastic facies under the load of overlying massive hyaloclastite breccia with dense clasts, sunken hyaloclasts and intrusion of hot magma into water-saturated volcaniclastic sand suggest that andesite volcaniclastic facies were poorly consolidated and wet at the emplacement of upper lavas and intrusions.

Repeated interbedding of beds of andesite volcaniclastic facies showing rapid vertical and lateral facies transitions suggest emplacement from contemporaneous granular flows rather than pulse events with significant time breaks in between. Contemporaneous emplacement is also in agreement with soft-sediment deformation structures exhibited by the fine volcaniclastic facies under the load of clasts in the coarse volcaniclastic facies.

5. Discussion

5.1. Emplacement mechanisms and eruption style of El Barronal complex

Andesite volcaniclastic facies have a wide spectrum of clast types that includes clasts derived from explosive eruptions (pumice, shards, crystals), clasts from underlying lavas (vesicular and dense) and minor reworked clasts from sources above wave base. These clasts may have been mixed together during syn-depositional remobilization of primary volcanic deposits by granular flows. They could also have been mixed together during explosive eruptions at sources above wave base and deposited by primary granular flows at deeper settings. Massive breccia lacks pumice clasts and glass shards, angular clasts from underlying lavas are dominant and the matrix is coarse (>2 cm). These features and the distribution of massive breccia and rapid transitions into fine volcaniclastic facies can be interpreted as massive breccia clasts derived from steam-driven explosions and deposited by primary granular flows during explosive eruptions with complex activity. Massive breccia could also have been deposited from granular flows triggered by repeatedly instability of lower lavas during explosive eruptions.

At El Barronal, the monomictic character of andesite volcaniclastic facies and the dominance of texturally fresh components (pumice clasts, glass shards, crystals and angular dense clasts) similar in composition to andesite lava facies suggest that volcaniclastic facies are syn-eruptive to lavas in a broad sense, i.e. both were emplaced during the same eruptive cycles. Several features suggest hiatus in the andesite volcanism between the cycles represented by andesite lavas and andesite volcaniclastic facies at different stratigraphic positions: $^{40}Ar/^{39}Ar$ ages of lavas, reworked clasts in andesite volcaniclastic facies, interbedding of andesite units with rhyolite lavas (Los

Genoveses Formation) and with carbonate and siliciclastic facies of epiclastic origin. Contact relations indicate that andesite volcaniclastic facies were unconsolidated at the time of emplacement of upper lavas and intrusion; furthermore, most clasts in the volcaniclastic facies were likely fragmented and mixed together by explosive eruptions. These features suggest that eruptive cycles at El Barronal started with explosive eruptions and continued with the emplacement of effusive lavas (Fig. 13). After emplacement of andesite lava, andesite volcanism stopped until a new cycle started again with explosive activity.

5.2. Facies model of El Barronal lavas. Comparison with felsic submarine and subaerial lavas, domes and cryptodomes

The association of facies observed in lava units of El Barronal leads to a general facies model consisting of an inner coherent core grading outward into hyaloclastite. Hyaloclastite is massive and made of dense clasts at the contact with coherent facies wheras toward the top and margins of lavas it is dominated by vesicular clasts and is layered, as a record of the original flow bands.

The overall structure of subaqueous lavas, domes and cryptodomes has been classified into three broad categories: A) inner coherent core grading into outer glassy and banded margin and into partly resedimented hyaloclastite breccia carapace (Pichler 1965; De Rosen-Spence et al. 1980; Yamagishi 1991; Goto and McPhie 1998, De Rita et al., 2001; Goto and Tsuchiya 2004; Stewart and McPhie 2003, 2006; Németh et al. 2008); B) inner coherent core grading into outer vesicular and banded margin and into partly resedimented carapace consisting of hyaloclastite pumice breccia (Kurokawa 1991; Allen et al. 2010); C) inner coherent core grading into an outer zone consisting of an alternation of vesicular bands and bands with jigsaw-fit to clast rotated hyaloclastite (Scutter et al. 1998).

The facies model for the El Barronal lavas is in agreement with those lavas having an outer vesicular/pumiceous zone. The overall facies architecture of the former ancient examples, including El Barronal, is roughly consistent with that of modern examples (Kato 1987; Allen et al. 2010). The main differences of El Barronal facies model with respect to examples with outer vesicular zones are: a) the vesicular zones at El Barronal grade inward into a thick hyaloclastite breccia made of dense clasts and then into a coherent core, whereas in the former examples the vesicular zones grade inward into a coherent core; b) at El Barronal, vesicularity is low (vesicles ≤40 vol. %) and vesicles are subspherical and poorly elongate with long/short axes ratios <5, whereas vesicles in the outer margins of lavas and domes in Ponza and Tadami district are highly elongate with long/short axes ratios >10 and vesicularity is probably higher (Kurokawa 1991; Scutter et al. 1998); c) resedimentation of outer vesicular zones produce volcaniclastic facies dominated vesicular non-pyroclastic clasts (Kurokawa 1991; Allen et al. 2010). This feature has not been observed at El Barronal.

The facies architecture of El Barronal lavas is also in agreement with the facies and textural stratigraphy of subaerial lavas and domes, which also show vesicular zones in the outermost parts (Fink and Manley 1987; Fink et al. 1992; Castro et al. 2002; Maeno and Taniguchi 2006).

At El Barronal, vesicular clasts derived from outer vesicular zones in the underlying lava units have been likely mixed together with the other components of volcaniclastic facies (pumice clasts, glass shards, crystals and dense rock clasts) by explosive eruptions rather than resedimented from the external vesicular zones of lavas during lava emplacement. The absence of resedimented deposits derived from the outer vesicular zones in El Barronal lavas, together with the preservation of thick vesicular zones grading into thick hyaloclastite breccia with dense clasts, suggests that quench fragmentation occurred nearly at the end of lava emplacement. In this view, the input of additional magma was minor and not able to trigger resedimentation of lava margins, allowing only for a local disorganization of the jigsaw-fit of clasts.

Conclusions

El Barronal Formation is a succession of lavas interbedded with volcaniclastic facies and minor siliciclastic and carbonate facies. Lavas and volcaniclastic facies are andesitic and have been emplaced in a shallow marine environment. Siliciclastic and carbonate facies are sedimentary rocks emplaced during periods of volcanic repose.

Coherent facies of El Barronal lavas include colonnade jointed and entablature jointed facies with rosette structures. Coherent facies is surrounded by hyaloclastite facies, which are volumetrically dominant and comprise massive to layered breccia with glassy clasts. Massive hyaloclastite breccia with dense clasts grades into massive hyaloclastite breccia with vesicular clasts and into layered hyaloclastite breccia. Layered hyaloclastite breccia consists of an alternation of bands of vesicular clasts and bands of dense clasts. Layered breccia reflects original flow bands defined by vesicularity. Hyaloclastite facies originated from quenching of hot magma in subaqueous conditions.

Volcaniclastic facies contain tube pumice clasts, crystals, glass shards, dense and vesicular clasts and minor reworked clasts from sources above wave base. Pumice clasts, crystals and shards are interpreted as produced during explosive eruptions. Dense clasts and vesicular clasts come from underlying lava units. Volcaniclastic facies are collectively interpreted as deposited from cold granular and non-cohesive flows with different grain size populations. Soft-sediment deformation structures in fine volcaniclastic facies at the contact to upper lavas suggest that volcaniclastic facies were unconsolidated and wet at time of emplacement of upper lavas. The former contact relation suggests that eruptions at El Barronal started with explosive eruptions and continued with effusive emplacement of lavas. $^{40}Ar/^{39}Ar$ ages of lavas, reworked clasts in volcaniclastic facies, interbedding of the andesite units formed by lavas and volcaniclastic facies with rhyolite lavas (Los Genoveses Formation) and with carbonate and siliciclastic facies of epiclastic origin suggests hiatus in the andesite volcanism.

El Barronal lavas consist of an inner coherent core grading outward into a hyaloclastite breccia of dense clasts and then into an outer vesicular zone. This facies architecture is similar to many felsic subaqueous and subaerial lavas, domes and cryptodomes described in the literature. However, some differences with subaqueous lavas and domes arise: vesicularity of the outer zone at El Barronal is lower; the outer zone at El Barronal grades into massive hyaloclastite breccia and not into coherent facies; resedimented facies of the outer vesicular zone has not been observed at El Barronal. The lack of resedimented deposits from the outer vesicular zones and the preservation of thick vesicular zones grading into thick hyaloclastite breccia with dense clasts, suggests that quench fragmentation at El Barronal occurred nearly at the end of lava emplacement.

Acknowledgements

This research has been funded by projects CGL2005-03511/BTE and HI2006-0073. We thank Parque Natural Cabo de Gata-Níjar for giving us permission to undertake this research. We also thank the participants of the Workshop held in May 2011 (http://www.ija.csic.es/cabodegata/) and Sandro Conticelli, Claudia Romano and Daniele Giordano for the fruitful discussions in the field. Ramon Julià helped with fossil identification. We thank Karoly Nemeth and Jocelyn McPhie for careful reviews.

References

Allen, S.R., Fiske, R.S., Tamura, Y., 2010. Effects of water depth on pumice formation in submarine domes at Sumisu, Izu-Bonin arc, western Pacific. Geology 38, 391-394.

Arribas, A. Jr., Cunningham, C.G., Rytuba, J.J., Rye, R.O., Kelly, W.C., Podwysocki, M.H., McKee, E.H, Tosdal, R.M., 1995. Geology, Geochronology, Fluid inclusions, and Isotope Geochemistry of the Rodalquilar Gold Alunite Deposit Spain. Economic Geology 90, 795-822.

Bear, A.N., Cas, R.A.F., 2007. The complex facies architecture and emplacement sequence of a Miocene submarine mega-pillow lava flow system, Muriwai, North Island, New Zealand. Journal of Volcanology and Geothermal Research 160, 1-22.

Brachert, T.C., Hultzsch, N., Knoerich, A.C., Krautworst, U.M.R., Stückrad, O.M., 2001. Climatic signature in shallow-water carbonates: high-resolution stratigraphic markers in carbonate build-ups (Late Miocene, southern Spain). Palaeogeography, Palaeoclimatology, Palaeoecology, 175, 211-237.

Cas, R.A.F., Allen, R.F., Bull, S.W., Clifford, B.A., Wright, J.V., 1990. Subaqueous, rhyolitic dome-top tuff cones: A model based on Devonian Bunga Beds, southeastern Australia and a modern analogue. Bulletin of Volcanology 52, 159-174.

Castro J., Cashman, K., Joslin, N., Olmsted, B., 2002. Structural origin of large gas cavities in the Big Obsidian Flow, Newberry Volcano. Journal of Volcanology and Geothermal Research 114, 313-33.

De Rosen-Spence, A.F., Provos,t G., Dimroth, E., Gochanauer, K., Owen, V., 1980. Archean subaqueous felsic flows, Rouyn- Noranda, Quebec, Canada and their Quaternary equivalents. Precambrian Research 12, 43-77.

De Rita, D., Giordano, G., Cecili, A., 2001. A model for submarine rhyolite dome growth: Ponza Island (central Italy). Journal of Volcanology and Geothermal Research 107, 221-239.

Di Battistini, G., Toscani, L., Iaccarino, S., Villa, I.M., 1987. K/Ar ages and the geological setting of calc-alkaline volcanic rocks from Sierra de Gata, SE Spain. Neues Jahrbuch für Mineralogie, Monatshefte, H. 8, 369-383.

Fernández Soler, J.M., 1987. Análisis e interpretación de los materiales volcánicos del Cerro de los Frailes (Cabo de Gata, Almería). Estudios Geológicos 43, 359-366.

Fernández Soler, J.M., 1992. El volcanismo calcoalcalino de la Sierra de Cabo de Gata (Almería). Estudio volcanológico y petrológico. PhD thesis, Universidad de Granada, pp 288.

Fernández-Soler, J.M., 2001. Volcanics of the Almeria Province. In: Mather, A., Martín, J.M., Harvey, A., Braga, J. (Eds.), A field guide to the Neogene Sedimentary Basins of the Almeria Province, South-East Spain. IAS Field Guide, Blackwell Science, Oxford, UK, 350, pp 58-88.

Fink, J.H., Manley, C.R., 1987. Origin of pumiceous and glassy textures in rhyolite flows and domes. In: Fink, J.H. (Ed.), Emplacement of Silicic Domes and Lava Flows: Special Paper Geological Society of America, 212, pp 77-88.

Fink, J.H., Anderson, S.W., Manley, C.R., 1992. Textural Constraints on Effusive Silicic Volcanism: Beyonf the Permeable Foam Model. Journal of Geophysical Research 97, 9073-9083.

Goto, Y., McPhie, J., 1998. Endogenous growth of a Miocene dacite cryptodome, Rebun Island, Hokkaido, Japan. Journal of Volcanology and Geothermal Research 84, 273-286.

Goto, Y., Tsuchiya, N., 2004. Morphology and growth style of a Miocene submarine dacite lava dome at Atsumi, northeast Japan. Journal of Volcanology and Geothermal Research 134, 255-275.

Head, J.W., Wilson, L., 2003 Deep submarine pyroclastic eruptions: theory and predicted landforms and deposits. Journal of Volcanology and Geothermal Research 121, 151-193.

Johnson, C.L., Franseen, E.K., Goldstein, R.H., 2005. The effects of sea level and paleotopography on lithofacies distribution and geometries in hetereozoan carbonates, south-eastern Spain. Sedimentology 52, 513-536.

Kato, Y. 1987. Woody pumice generated with submarine eruption. Journal of the Geological Society of Japan 93, 11-20.

Kurokawa, A., 1991. Formation of felsic pumiceous hyaloclastites: a case study from Tadami district, Fukushima Prefecture, Japan. Journal of Mineral Petrology and Economic Geology 86, 439-458.

Maeno, F., Taniguchi, H., 2006. Silicic lava dome growth in the 1934-1935 Showa Iwo-jima eruption, Kikai caldera, south Kyushu, Japan. Bulletin of Volcanology 68, 673-688.

Manga, M., Patel, A., Dufek, J. 2011. Rounding of pumice clasts during transport: field measurements and laboratory studies. Bulletin of Volcanology 73, 321-333.

Martí, J., Soriano, C., Dingwell, D.B. 1999. Tube pumices as strain markers of the ductile-brittle transition during magma fragmentation. Nature 402, 650-653.

Martín, J.M., Braga, J.C., Betzler, C., Brachert, T.C., 1996. Sedimentary model and high-frequency cyclicity in a Mediterranean, shallow-shelf, temperate-carbonate environment (uppermost Miocene, Agua Amarga Basin, Southern Spain). Sedimentology 43, 263-277.

McPhie, J., Doyle, M., Allen, R.L., 1993. Volcanic Textures: a guide to the interpretation of textures in volcanic rocks. Centre for Ore Deposits and Exploration Studies, University of Tasmania, pp 198.

Montenat, C., Ott d'Estevou, P., 1990. Eastern Betic Neogene basins-A Review. Doc. Et Trav. Igal. 12-13, 9-15.

Montgomery, P., Farr, M.R., Franseen, E.K., Goldstein, R.H., 2001. Constraining controls of carbonate sequences with high-resolution chronostratigraphy: Upper Miocene, Cabo de Gata region, SE Spain. Palaeogeography, Palaeoclimatology, Palaeoecology 176, 11-45.

Németh, K., Pécskay, Z., Martin, U., Gméling, K., Molnár, F., Cronin, S.J., 2008. Hyaloclastites, peperites and soft-sediment deformation structures of a shallow subaqueous Miocene rhyolitic dome-cryptodome complex, Pálháza, Hungary. In: Thomson, K., Petford, N. (Eds.), Structure and emplacement of high-level magmatic systems: Geological Society London, Special Publications 302, 63-86.

Páez Carrión, A., Sánchez Soria, P., 1965. Vulcanología del Cabo de Gata, entre San José y Vela Blanca. Estudios Geológicos XXI, 223-246.

Pedrera, A., Marín-Lechado, C., Galindo-Zaldívar, J., Rodríguez-Fernández, L.R., Ruiz-Constán, A. 2006. Fault and fold interaction during development of the Neogene-Quaternary Almería-Níjar basin (SE Betic Cordilleras). In: Moratti, G., Chalouan, A. (Eds.), Tectonics of the Western Mediterranean and North Africa: Geological Society, London, Special Publications, 262, 217-230.

Reicherter, K., Hübscher, C., 2007. Evidence for a sea floor rupture of the Carboneras Fault Zone (southeastern Spain): Relation to the 1522 Almeria earthquake? Journal of Seismolology 11, 15-26.

Pichler, H., 1965. Acid hyaloclastites. Bulletin Volcanologique 28, 293-310.

Polacci, M., Pioli, L., Rosi, M. 2003. The plinian phase of the Campanian Ignimbrite eruption (Phelgrean Fields, Italy): evidence from density measurements and textural characterization of pumice. Bulletin of Volcanology 65.

Rosi, M., Landi, P., Polacci, M., Di Muro, A., Zandomeneghi, D. 2004. Role of conduit shear on ascent of the crystal-rich magma feeding the 800-year eruption of Quilotoa (Ecuador). Bulletin of Volcanology 66, 307-321.

Sáenz de Galdeano, C., Vera, J.A., 1992. Stratigraphic record and palaeogeographical context of the Neogene basins in the Betic Cordillera. Basin Research 4, 21-36.

Scotney, P., Burgess, R., Rutter, E., 2000. $^{40}Ar/^{39}Ar$ age of the Cabo de Gata volcanic series and displacements on the Carboneras fault zone, SE Spain. Journal of the Geological Society, London 157, 1003-1008.

Scutter, C.R., Cas, R.A.F., Moore, C.L., de Rita, D., 1998. Facies architecture and origin of a submarine rhyolitic lava-flow dome complex, Ponza, Italy. Journal of Geophysical Research 103, 27, 551-27,566.

Serrano, F., 1992. Biostratigraphic control of Neogen volcanism in Sierra de Gata (south-east Spain). Geologie Mijnbow 71, 3-14.

Skilling, I.P, White, J.D.L., McPhie, J., 2002. Peperite: a review of magma sediment-mingling. Journal of Volcanology and Geothermal Research 114, 1-17.

Stewart, A.L., McPhie, J., 2003. Internal structure and emplacement of an Upper Pliocene dacite cryptodome, Milos Island, Greece. Journal of Volcanology and Geothermal Research 124, 129-148.

Stewart, A.L., McPhie, J., 2006. Facies architecture and Late Pliocene-Pleistocene evolution of a felsic volcanic island, Milos, Greece. Bulletin of Volcanology 68, 703-726.

Yamagishi, H., 1991. Morphological and sedimentological characteristics of the Neogene submarine coherent lavas and hyaloclastites in Southwest Hokkaido, Japan. Sedimentary Geology 74, 5-23.

Yamagishi, H., Dimroth, E., 1985. A comparison of Miocene and Archean rhyolite hyaloclastites: evidence for a hot and fluid rhyolite lava. Journal of Volcanology and Geothermal Research 23, 337-355.

List of figures

Table 1. Ar^{40}/Ar^{39} summary data for andesite lavas of El Barronal Formation.

Fig. 1. Geological map of the Betic-Rif Orogen in the Western Mediterranean. The enlarged inset shows details of the Almeria-Níjar basin and the Cabo de Gata volcanic zone and location of Fig. 2.

Fig. 2. Geological and facies map of El Barronal area showing the location of stratigraphic logs in Figure 3 and cross-section in Figure 4.

Fig. 3. Simplified stratigraphic logs of El Barronal Formation and stratigraphic correlations of andesite lava units and andesite volcaniclastic facies. Lava units are numbered 1 to 5 in stratigraphic order.

Fig. 4. Schematic cross-section along the coast showing lava units and facies types of El Barronal Formation.

Fig. 5. A: Entablature columnar-jointed facies in lava unit 3 (Ej) grades downward into massive hyaloclastite breccia with dense clasts (Da) and is underlain by andesite volcaniclastic facies. B: Rosette structures in lava unit 3 (R) grade into massive hyaloclastite breccia with dense clasts (Da). See Figure 2 for location of photographs.

Fig. 6. A: Field sketch of the lithofacies of lava unit 1 and the contact relation with overlying bedded andesite volcaniclastic facies. Ej: Entablature columnar-jointed facies with columnar joints shallowly dipping to the NE; Da: Massive hyaloclastite breccia

with dense clasts; Va: Massive hyaloclastite breccia with vesicular clasts; Cv: Cross-bedded crystal-rich volcaniclastic facies. See Figure 3 for stratigraphic location. B: Photomicrograph (plane polarised light) of massive hyaloclastite breccia with vesicular clasts showing vesicles (v) deformed against neighbour vesicles. Pl is plagioclase phenocryst. C: Detail of the contact between massive hyaloclastite breccias with dense clasts (Da) and vesicular clasts (Va). D: Domains of cross-bedded crystal-rich volcaniclastic facies (Cv) within massive hyaloclastite breccia with vesicular clasts (Va). See text for description of contact features.

Fig. 7. A: Layered hyaloclastite breccia of lava unit 3 with subvertical undulating bands of vesicular clasts (Vc) and dense clasts (Dc). B: Detail of the jigsaw fit within bands of dense clasts. C: Field sketch of the contact between layered hyaloclastite breccia with subvertical bands of lava unit 3 and subhorizontal beds of the overlying andesite volcaniclastic facies. Volcaniclastic facies consists of thinly bedded fine tuffaceous sandstone (Fbt) and is overlain by massive hyaloclastite breccia with dense clasts (Da) of lava unit 4. See Figure 4 for location.

Fig. 8. A: Layered hyaloclastite breccia dipping gently to the ESE with bands of vesicular clasts (Vc) and bands of dense clasts (Dc). See Figure 4 for location. B: Photomicrograph (plane polarised light) of a band of vesicular clasts with elongated vesicles (v) deformed around crystals. The groundmass surrounding plagioclase (Pl) and pyroxene (Py) crystals is dominantly vesicular.

Fig. 9. A: Massive breccia (Mb) interbedded and grading into thinly bedded fine tuffaceous sandstone (Fbt) in the andesite volcaniclastic succession overlying lava unit 3. B: Detail of the contact in Figure 9A. Thinly bedded fine tuffaceous sandstone contains outsized vesicular clasts (Vc) and shows distorted lamination under the load of dense clasts (Dc) of the massive breccia. Arrows point to low-angle truncations. C:

Lava unit 3 with entablature columnar-jointed facies (Ej) grading into massive hyaloclastite breccia with dense clasts (Da) pinches out laterally to the W (toward the viewer) into andesite volcaniclastic facies. Volcaniclastic facies show rapid vertical and lateral changes between beds of massive breccia (Mb) and beds of thinly bedded fine tuffaceous sandstone (arrows). See Figure 2 for location of photograph.

Fig. 10. A: Diffusely bedded pumice-rich breccia with outsized dense clasts showing contrasting difference in rounding. B: Photomicrograph (plane polarised light) of diffusely bedded pumice-rich breccia with pumice clasts (P) showing random orientations of the tube vesicles and the clast edges parallel and at high angles to the tubes. C: Photomicrograph (plane polarised light) of diffusely bedded pumice-rich breccia. Tube pumice clast (P); Dense rock clast (Dr); cuspate and bubble wall shards (S).

Fig. 11. A: Photomicrograph (plane polarised light) of cross-bedded crystal-rich sandstone with rounded dense rock clasts (Dr). B Photomicrograph (plane polarised light) of thinly bedded fine tuffaceous sandstone with platy glass shards (s) and blocky shape crystal fragments (b).

Fig. 12. Stratigraphic log and contact relations of the volcaniclastic facies located between lava unit 2 and 3. See Figure 5 for location. Da: Massive breccia with dense clasts; Fbt: thinly bedded fine tuffaceous sandstone. Arrows point to thin beds distorted under the load of a dense clast of lava unit 3 sunken into the thinly bedded fine tuffaceous sandstone.

Fig. 13. Schematic evolution of the andesite volcanism, the processes and the resultant facies architecture during the El Barronal Formation. For simplicity only explosive eruptions at the starting of andesite volcanism in cycle II have been represented (see text for further discussion).

Dear Prof. Wilson,

Please, find attached the revised version of the ms entitled **Facies architecture, emplacement mechanisms and eruption style of the submarine andesite El Barronal complex, Cabo de Gata, SE Spain** by Soriano et al. for submission to JVGR.

We have followed nearly all the suggestions made by both reviewers in their annotated copies, including references (some of them have been added and some others omitted), figure citations, minor modification in figures, and text rewording.

Now we comment about the points addressed by reviewer #2.

1. The rocks studied in this ms were already characterized as subaqueous lavas with coherent and hyaloclastite facies in previous studies undertaken in Cabo de Gata. It is clearly stated in the revised version we submit now (lines 126-129). This is the current description and interpretation for these rocks and we follow it in the ms. Eventually, we argue with it later on in the text in those cases where we find evidence to do it (for example lava unit 1). We believe that with the organization and terms we propose now the reader has a more informative and clear idea of about what is dealing with in the text. Our previous terms created some confusion (indeed, it was not clear to reviewer #2 if the facies described in sections 4.1 and 4.4 of the previous version were the same or not) and it was equally confusing and ambiguous our designation of "clastic lava facies" or the reviewer's proposal of "breccia facies" for section 4.3 of the previous version.
2. Description of groundmass texture has been added to the text to reinforce interpretation of quenching.
3. The section on bedded volcaniclastic facies has been partly rewritten to build up more sound interpretations. In particular, fragmentation, transport and depositional processes of these facies have been evaluated independently.
4. The description of the contact relation of lava unit 1 has been improved to support the interpretation proposed.
5. The comparison of El Barronal lavas to other lavas and domes has been shortened and the sentence about endogenous growth has been omitted.
6. The conclusions have been rewritten in accordance with the changes made in the text.

We hope that now the ms is suitable for publication in JVGR.

Yours sincerely,

Carles Soriano

Table
Click here to download Table: Table 1.xls

Summary of $^{40}Ar/^{39}Ar$ incremental heating experiments

						Weighted Mean Analysis				Isochron Analysis		
Sample	Rock type	Unit	Location	Material	K/Ca total	^{39}Ar %	MSWD	Age (Ma) ± 2 σ	N	$^{40}Ar/^{36}Ar$ ± 2 σ	MSWD	Age (Ma) ± 2 σ
CG303	coherent lava	El Barronal Fm	36°44'18.71"N 2° 06'58.72"W	groundmass	1.253	91.3	0.44	**12.19 ± 0.08**	8 of 10	291.9 ± 6.0	0.28	12.23 ± 0.10
CG304	coherent lava	El Barronal Fm	36°44'18.48"N 2° 07'03.78"W	groundmass	1.001	61.0	0.73	**12.67 ± 0.05**	4 of 10	295.2 ± 2.0	1.05	12.68 ± 0.08

All ages calculated using the decay constants of Steiger and Jäger ($\lambda_{40K} = 5.543 \times 10^{-10}$ yr^{-1})
J-value calculated relative to 28.34 Ma for the Taylor Creek sanidine
Age in **bold** is preferred

Figure
Click here to download high resolution image

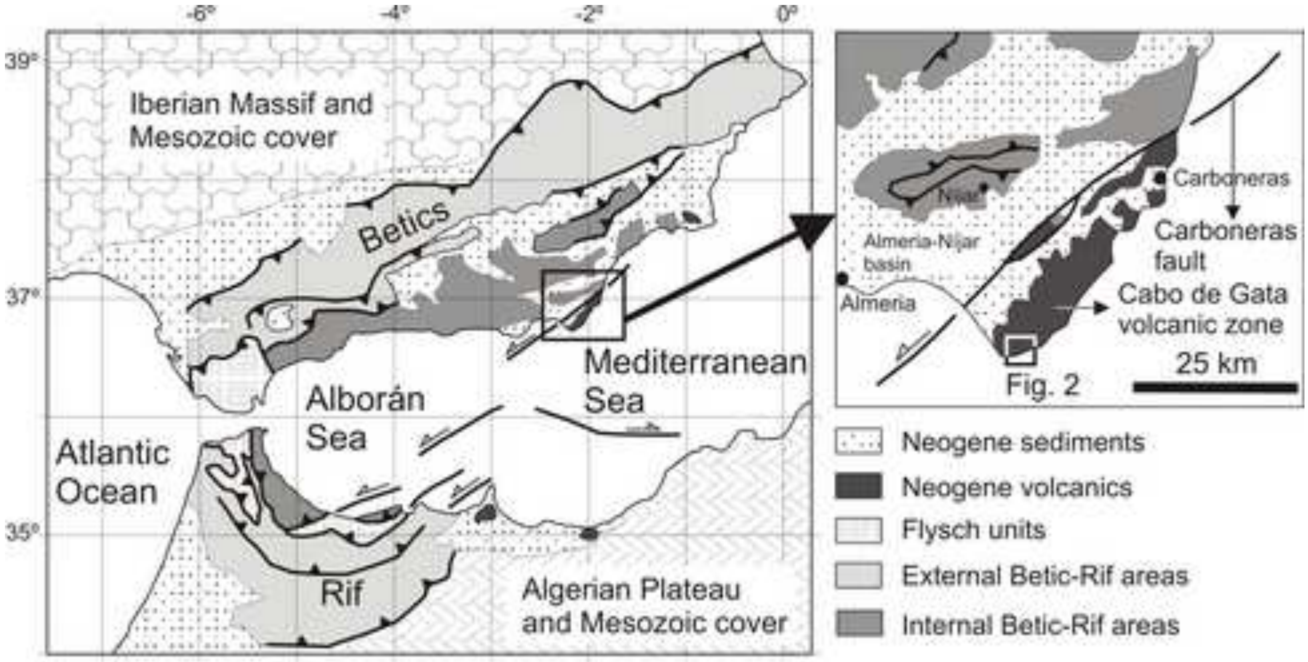

Fig. 1

Figure
Click here to download high resolution image

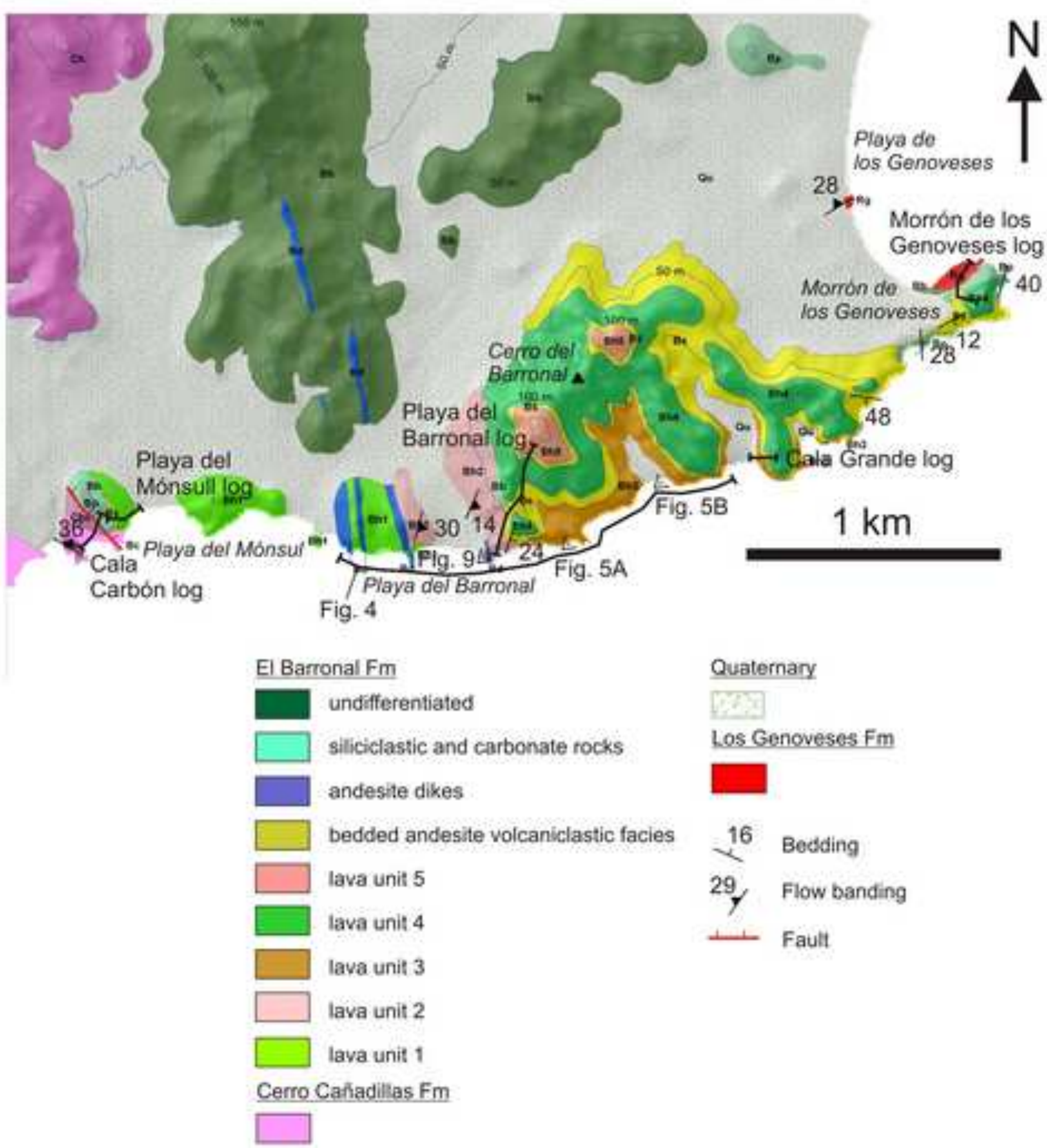

Fig. 2

Figure
Click here to download high resolution image

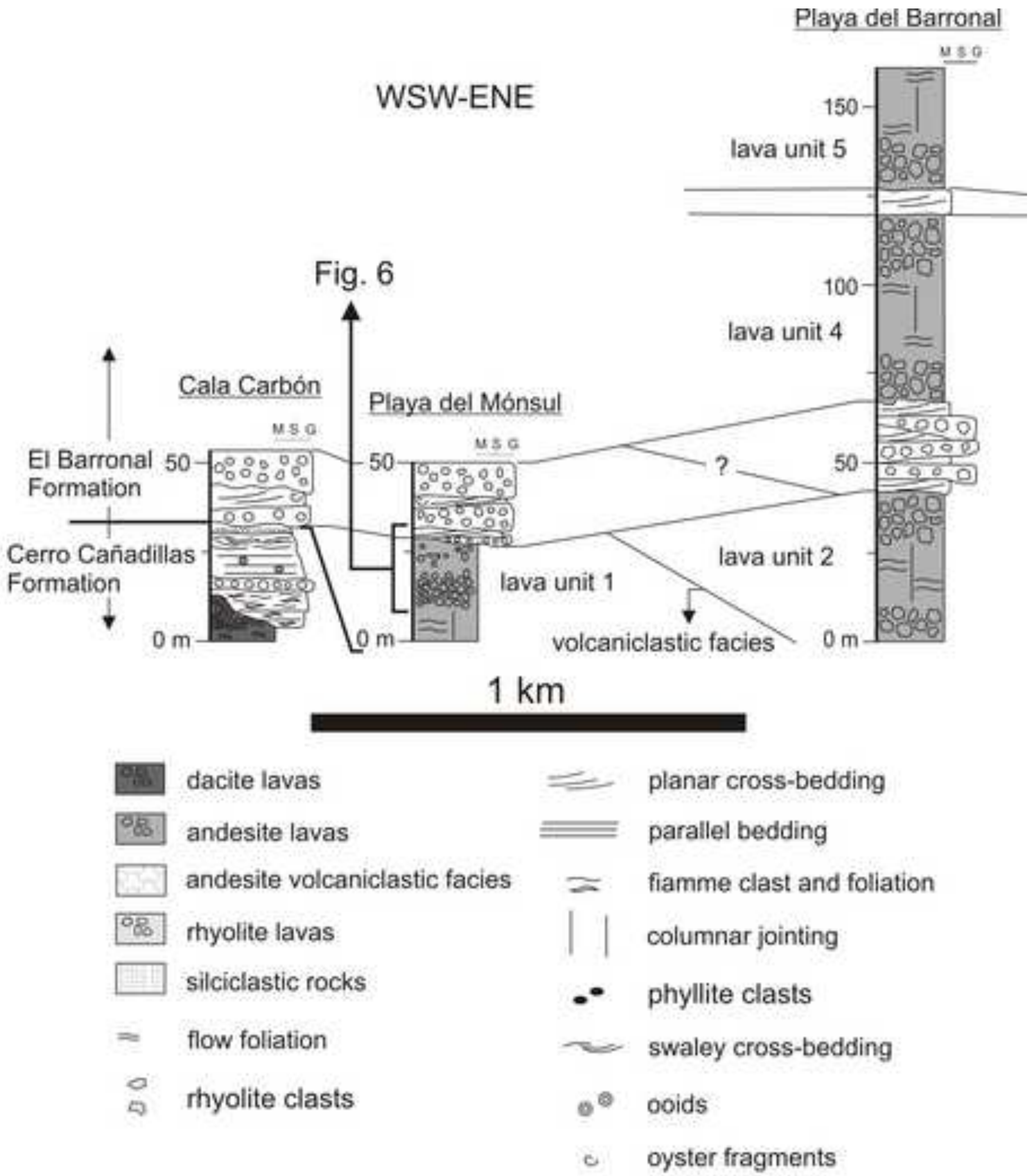

Fig. 3

Figure

Click here to download high resolution image

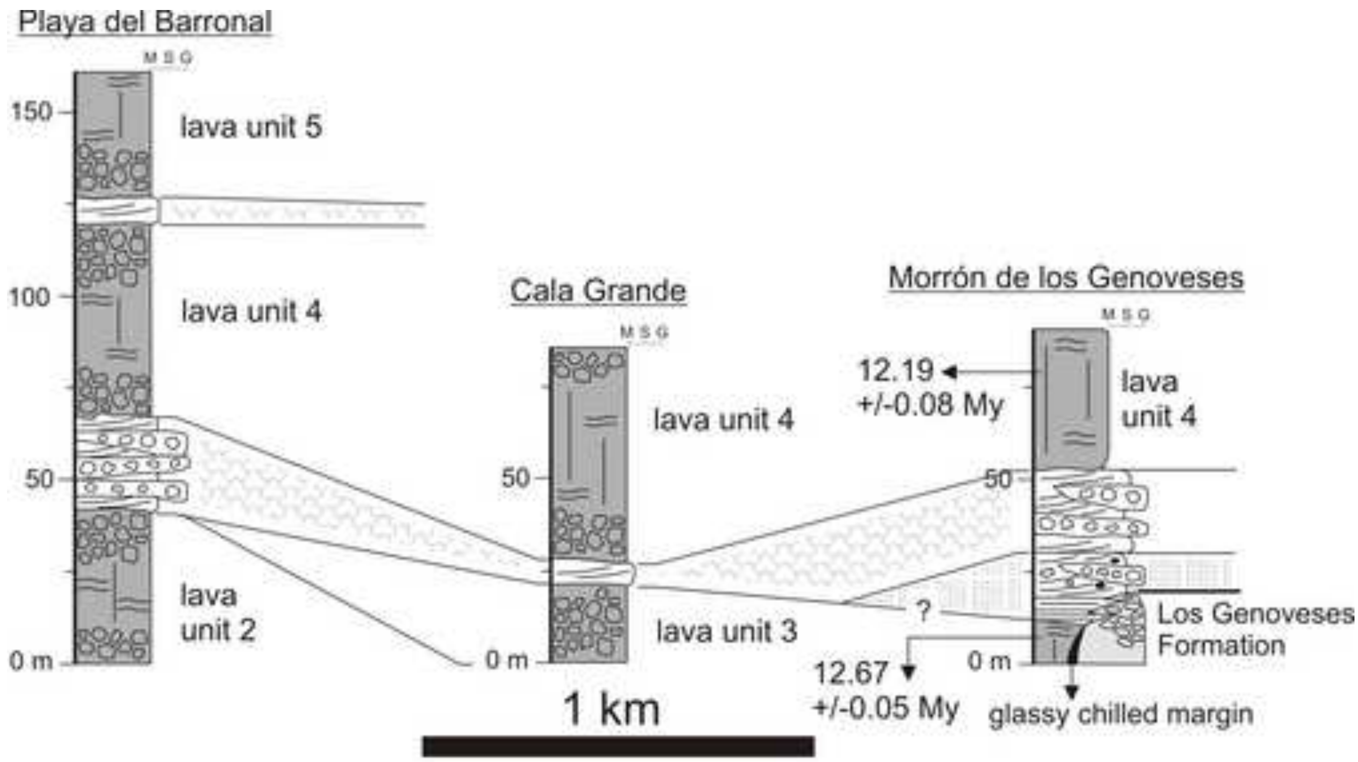

Fig. 3 (cont.)

Figure
Click here to download high resolution image

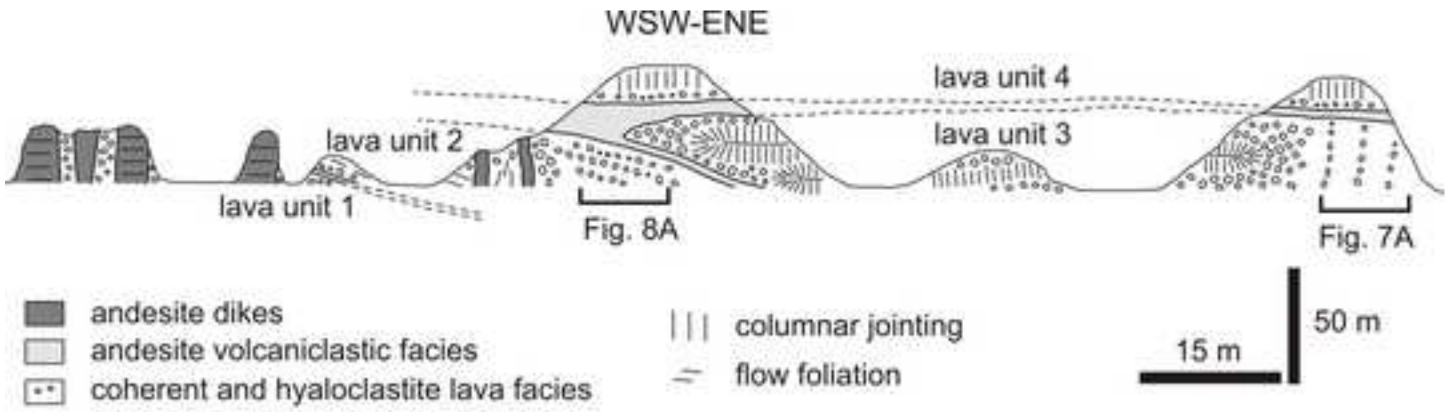

Fig. 4

Figure
Click here to download high resolution image

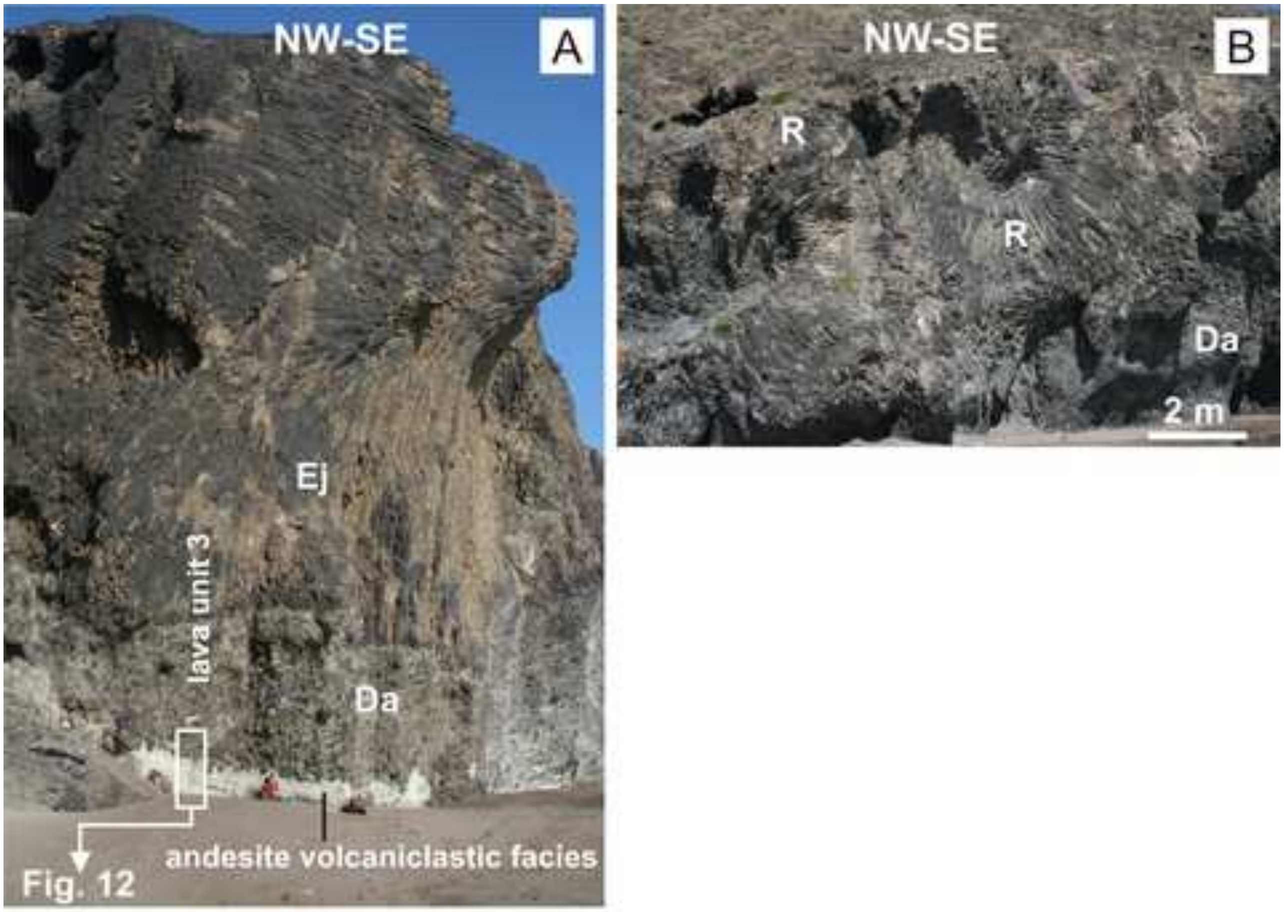

Fig. 5

Figure
Click here to download high resolution image

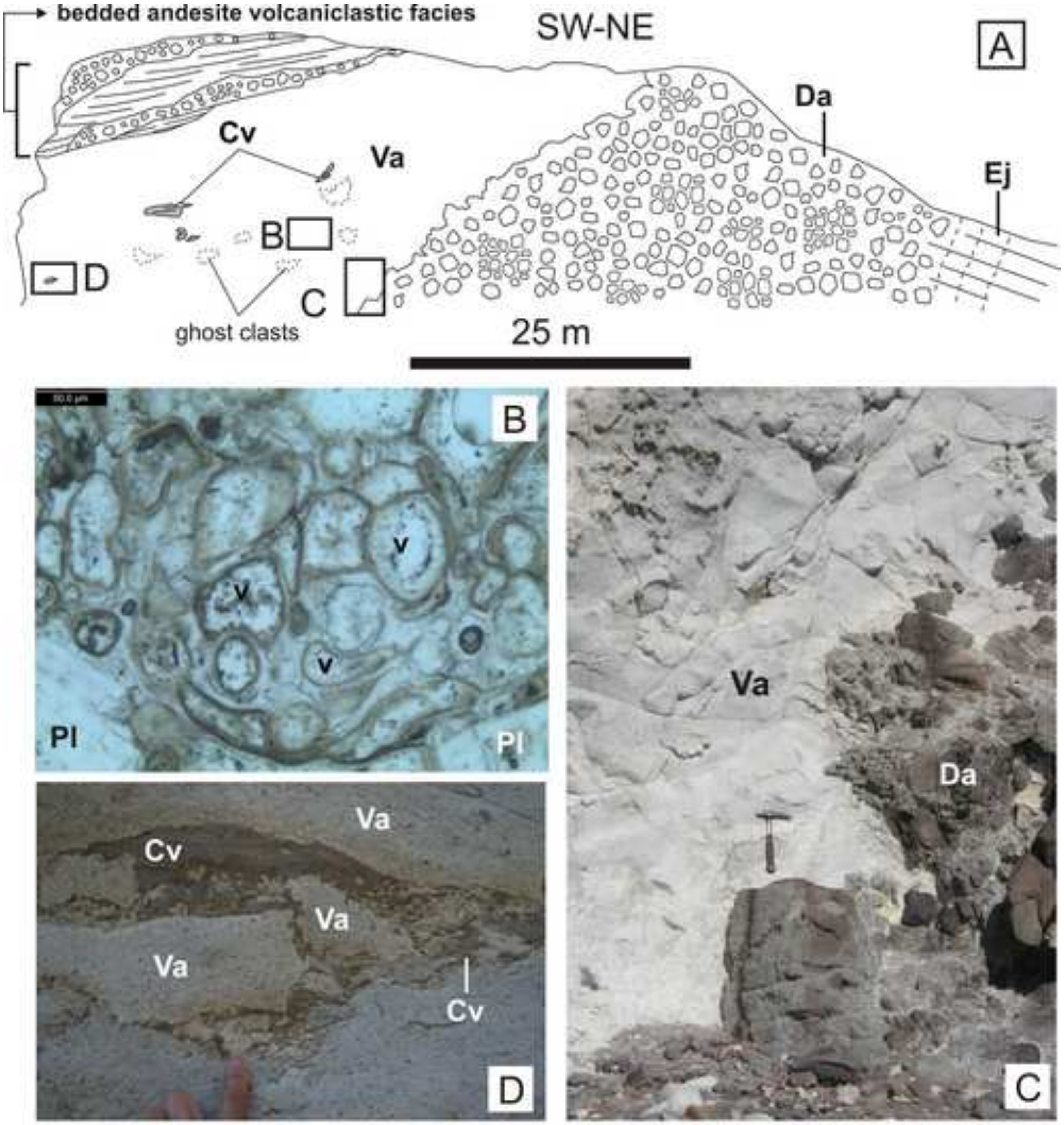

Fig. 6

Figure
Click here to download high resolution image

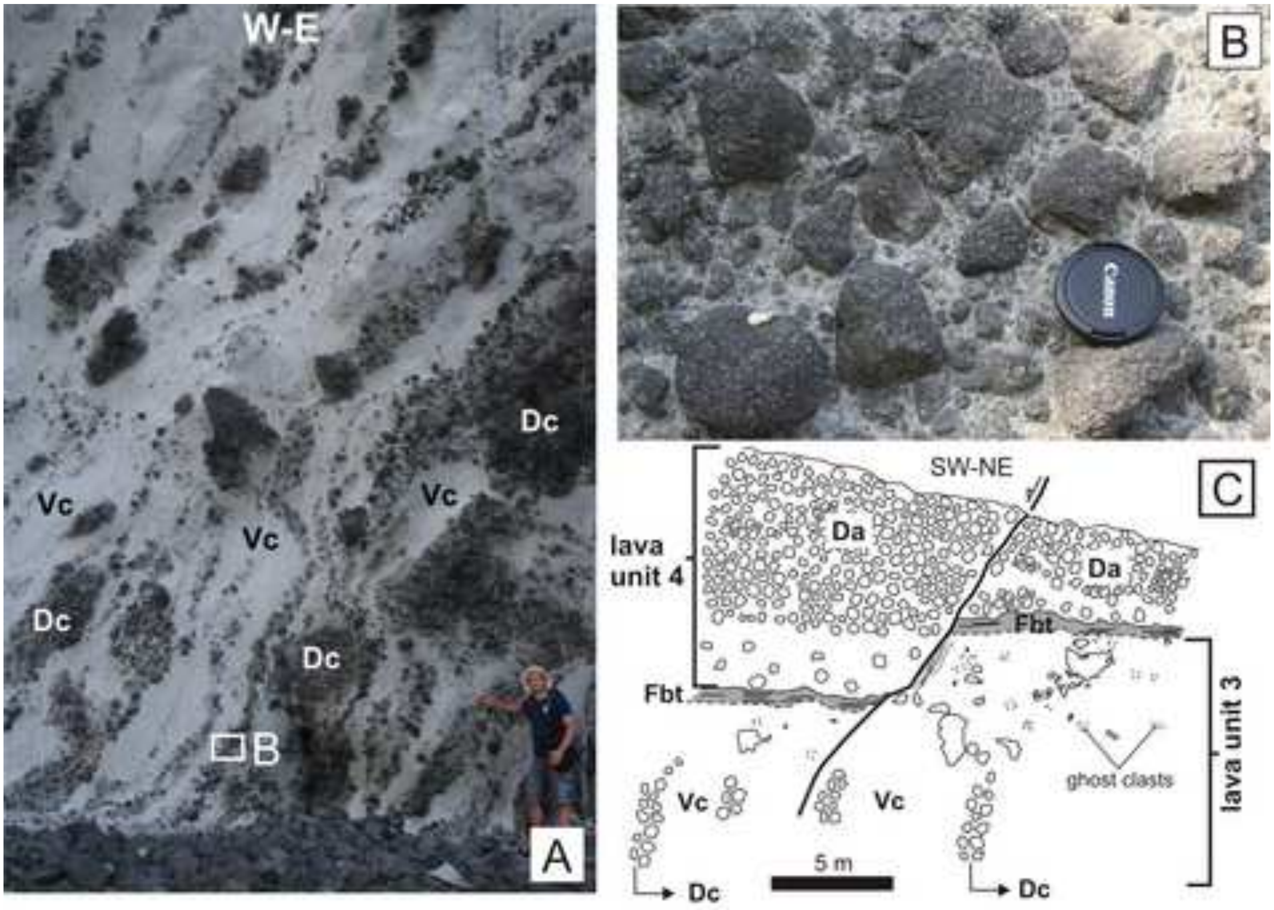

Fig. 7

Figure
Click here to download high resolution image

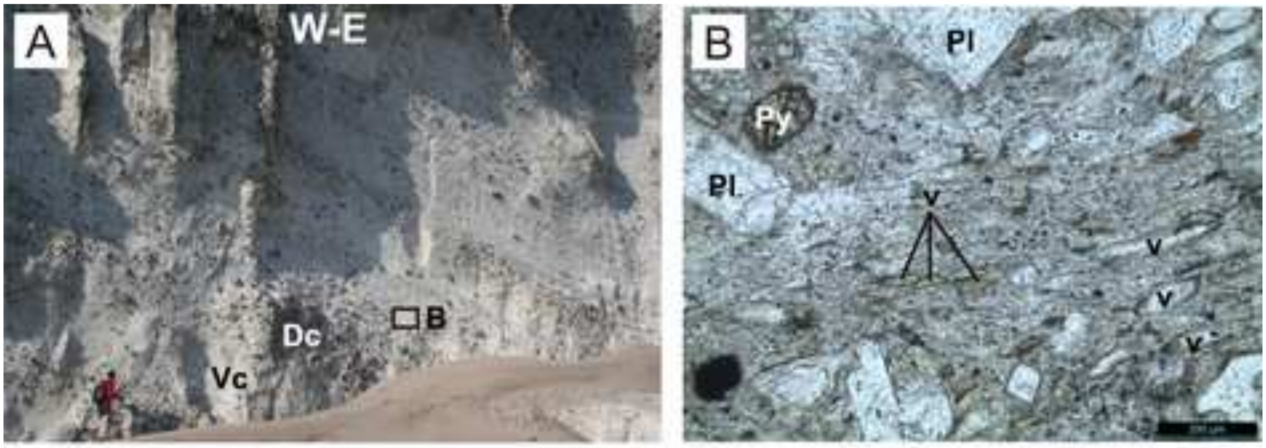

Fig. 8

Figure

Click here to download high resolution image

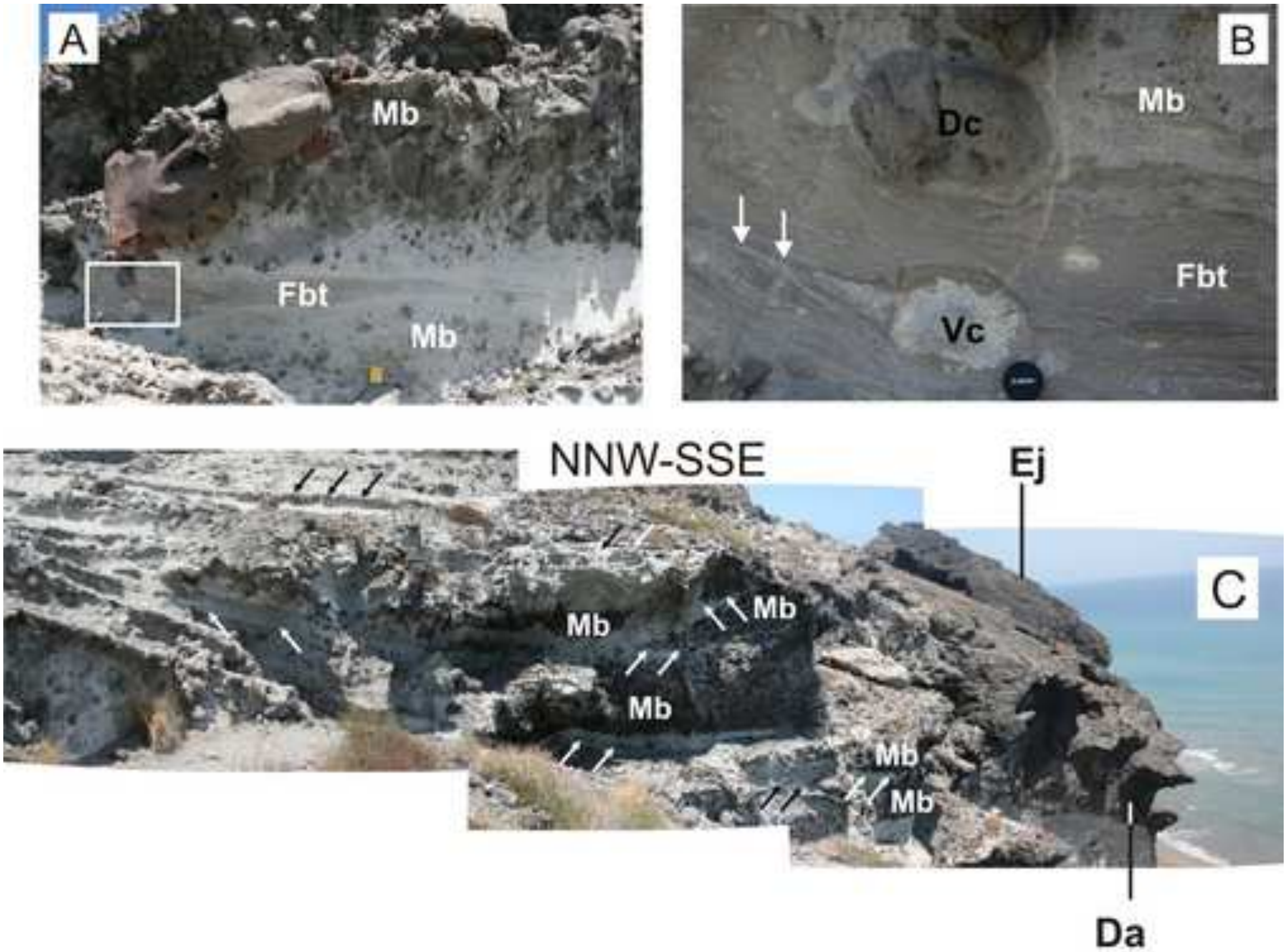

Fig. 9

Figure
Click here to download high resolution image

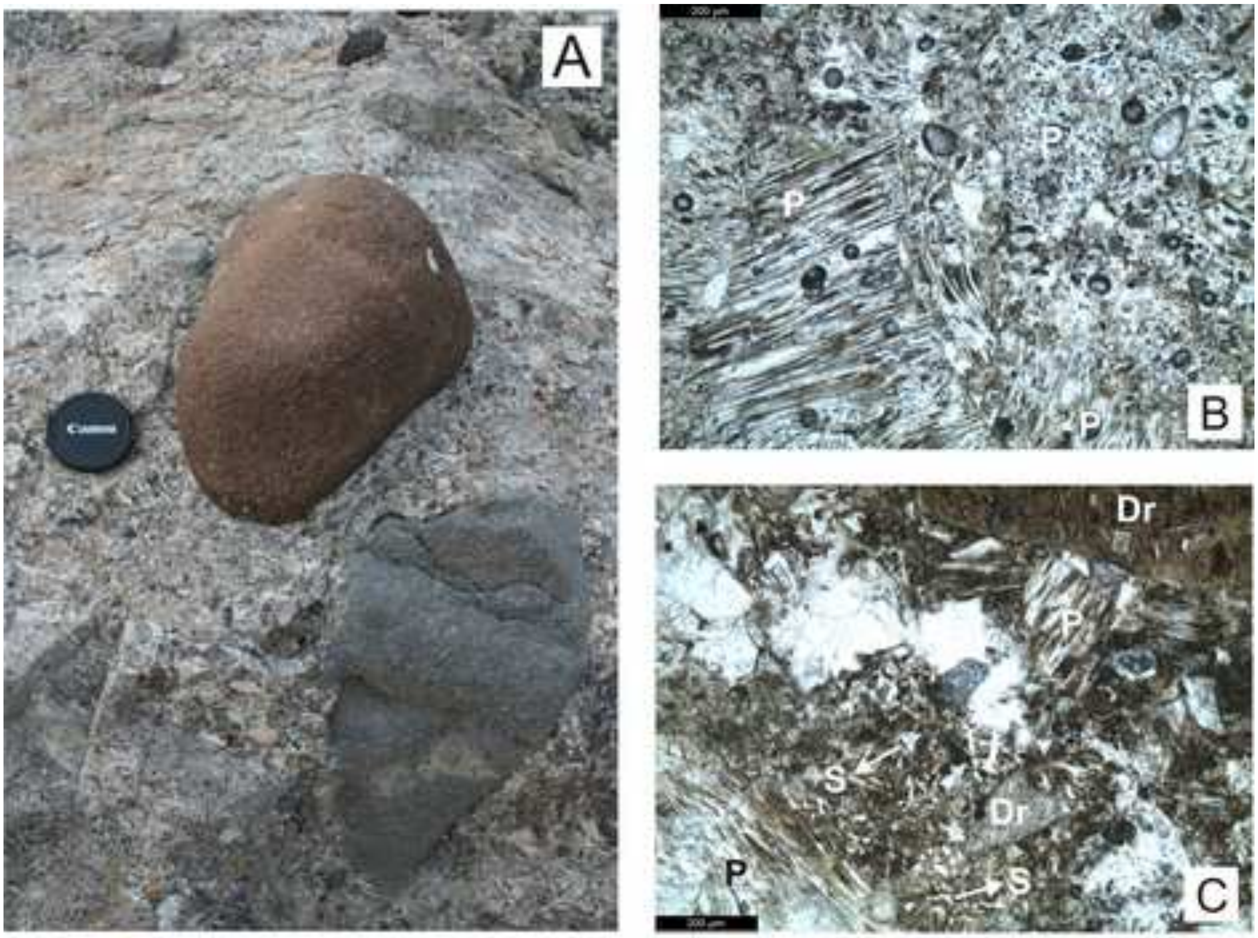

Fig. 10

Figure
Click here to download high resolution image

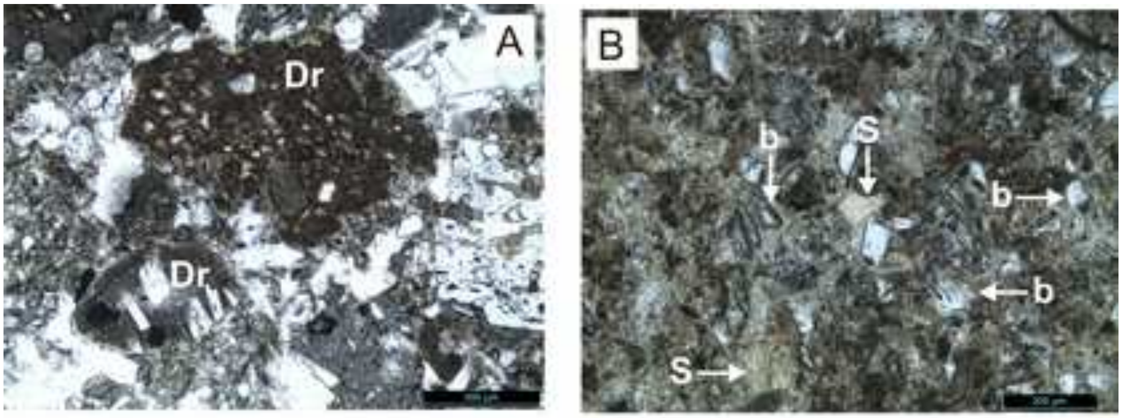

Fig. 11

Figure
Click here to download high resolution image

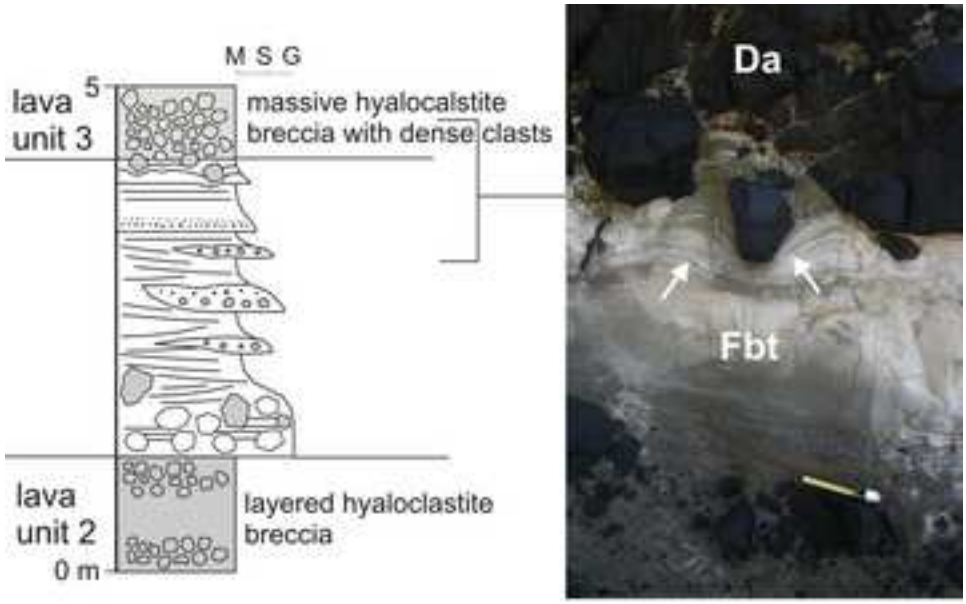

Fig. 12

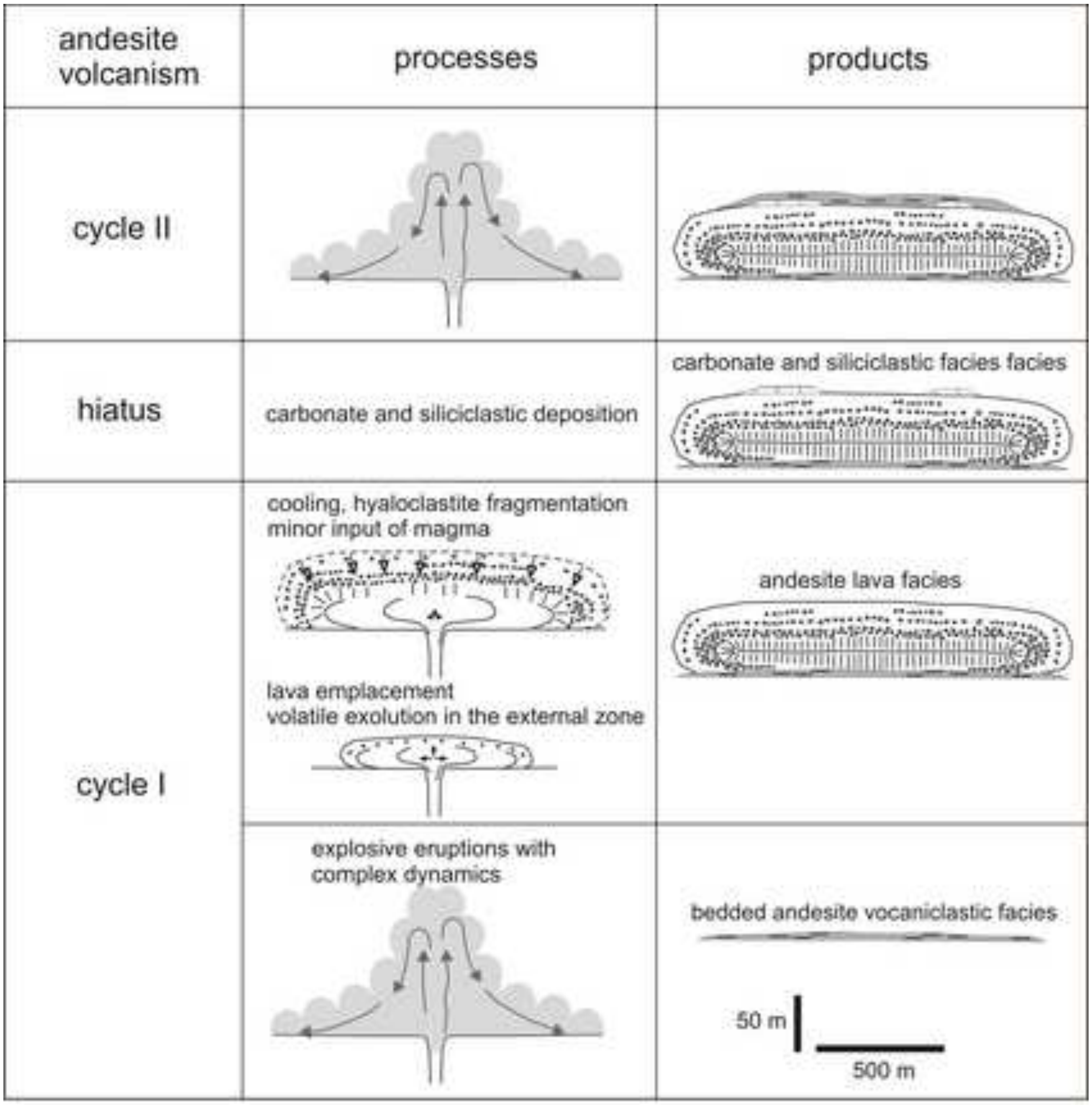
andesite volcanism
processes
products
cycle II
hiatus
carbonate and siliciclastic deposition
carbonate and siliciclastic facies facies
cycle I
cooling, hyaloclastite fragmentation
minor input of magma
andesite lava facies
lava emplacement
volatile exolution in the external zone
explosive eruptions with
complex dynamics
bedded andesite vocaniclastic facies
50 m
500 m

Fig. 13